Geometrical properties of parafermionic spin models

Marco Picco, Raoul Santachiara, Alberto Sicilia

Geometrical properties of parafermionic spin models.

M. Picco[1], R. Santachiara[2] and A. Sicilia[1]
[1] *LPTHE*[*], *Université Pierre et Marie Curie-Paris6 and*
Université Denis Diderot-Paris7
Boîte 126, Tour 24-25, 5 ème étage,
4 place Jussieu, F-75252 Paris CEDEX 05, France,
e-mail: picco,sicilia@lpthe.jussieu.fr.
[2] *LPTMS,* [‡]*, Université Paris-Sud*
Bâtiment 100
91405 Orsay, France.
e-mail: santachi@lpt.ens.fr.

(Dated: December 18, 2008)

ABSTRACT

We present measurements of the fractal dimensions associated to the geometrical clusters for Z_4 and Z_5 spin models. We also attempted to measure similar fractal dimensions for the generalised Fortuyin Kastelyn (FK) clusters in these models but we discovered that these clusters do not percolate at the critical point of the model under consideration. These results clearly mark a difference in the behaviour of these non local objects compared to the Ising model or the 3-state Potts model which corresponds to the simplest cases of Z_N spin models with $N = 2$ and $N = 3$ respectively. We compare these fractal dimensions with the ones obtained for SLE interfaces.

1 Introduction

The geometrical description of phase transitions has a long history [1]. The existence of exactly solved models and, most importantly, the richness of the conformal symmetry in two dimensions (2D), make the two-dimensional statistical systems an ideal framework to study this problem. The critical points of 2D systems can be classified using conformal field theories (CFTs) which also provide a powerful approach to compute exactly correlation functions of local operators. The first major breakthrough in the study of conformally invariant interfaces in 2D critical models has come from the introduction of the so-called Coulomb-gas (CG) formalism [2]. When a model is provided with a CG description, the combination of CG and CFT techniques allow the exact computation of geometrical exponents which characterize the fractal shape of critical interfaces. This has been done for a variety of critical statistical models as critical percolation, self-avoiding walks, loop erased random walks, etc. All these models are associated to the so called minimal CFTs or equivalently to the critical phases of $O(n)$ models [2]. Using

[*]Unité mixte de recherche du CNRS UMR 7589.
[‡]Unité mixte de recherche du CNRS UMR 8626.

the CG description of the $O(n)$ model, the fractal dimension (and more generally all the multi-fractal scaling exponents) of critical interfaces has been exactly computed [3, 4]. A remarkable recent development in the study of critical interfaces in 2D systems came with the introduction of a conceptually new approach based on the so called Schramm-Loewner evolutions (SLEs), which are growth processes defined via stochastic evolution of conformal maps [5, 6, 7]. Again, the SLE approach, which provides a geometrical description of CFT, is completely understood only in the case of minimal CFTs [8, 9, 10].

The minimal CFTs are constructed by demanding the correlation functions to satisfy the conformal symmetry alone and they represent a small set of CFT theories. There are many other interesting CFTs, called extended CFTs, which describe many condensed matter and statistical problems which are characterized in general by some internal symmetry such as, e.g., the $SU(2)$ spin-rotational symmetry in spin chains [11] or replica permutational symmetry in disordered systems [12, 13]. Despite all the recent activity and progress, the geometrical properties of such extended CFTs are in general not understood. In this respect some progress has been done by studying the connection between SLE and Wess-Zumino-Witten models, i.e. CFTs with additional Lie-group symmetries [14, 15], and by defining loop models associated to some extended CFTs [16, 17, 18, 19, 20]. In this direction of investigation, a very interesting family of critical models are the Z_N spin models (defined below) i.e. a lattice of spins which can take N-values. The nearest-neighbor interaction defining the model is invariant under a Z_N cyclic permutation of the states. For $N = 2$ and $N = 3$ these models correspond to the well known Ising and three-states Potts model whose critical points are described by minimal CFTs. For $N \geq 4$ instead, the models admit critical points described by parafermionic theories which are extended CFTs where the role of the $Z(N)$ symmetry beside the one of conformal symmetry must be taken into account. The geometrical properties of Z_N spin models are for many aspects unknown and their study are expected to provide general deep insights on the geometrical description of extended CFTs.

In a recent work [21] one of the authors proposed an extension of the concept of SLE to the case of the Z_N parafermionic theory. An SLE interface is associated to the (conformal) boundary condition which generates it. Considering the Z_N spin model on a bounded domain, say the half-plane for instance, and specifying a particular boundary condition, an SLE interface was identified as the boundary of the geometrical cluster connected to the negative axis [21]. By the term geometrical cluster we mean the cluster which connects spins with equal value. This interface was further studied in [22] where the corresponding fractal dimension has been shown to be in agreement with the CFT predictions in [21]. Nevertheless by considering other boundary conditions, we obtained different results for the fractal dimensions of the corresponding interfaces in the case of the Z_N spin model with $N \geq 4$ [23]. This is at odd from results for the Potts models for which a single fractal dimension for the geometrical interface (i.e. the boundary of the geometrical cluster) is obtained [24].

The present work is thus motivated by determining the bulk fractal dimension, *i.e.*the fractal dimension associated to finite clusters in the model. To be more precise, we will consider in this work the fractal dimensions obtained by constructing the distribution of all the finite closed geometrical clusters. As we will show later, the geometrical clusters do percolate at the critical point of the Z_N spin model in the sense that there is a one large cluster which span the entire lattice at the critical point. The distribution of the

smallest clusters can then be used to define a set of exponents as is the case in percolation theory and from these exponents one can determine the fractal dimension.

At this point, one needs to provide some explanation on why we concentrate on the geometrical clusters. It is well known that while the geometrical clusters do percolate at the critical point in two dimensional Potts models, they do not contain the physical information of the model considered. For example the exponents obtained from the geometrical clusters of the two dimensional Ising model are not the exponents of the Ising model [25, 26]. These exponents are in fact encoded in some other objects, the FK clusters. Obviously, the FK clusters must also percolate at the critical point. That the geometrical clusters percolate for the same critical temperature as for the FK clusters is true for the Potts models in two dimensions but is not a general result. In three dimensions for the Ising model, the percolation of the Ising model occurs at a different temperature [27,28]. In fact, one has no reason to expect that the geometrical clusters do percolate at the critical point for any two dimensional model. That it is the case for the Potts models can be traced back to the existence of some duality relation. In particular, in the correspondent CG formulation of the Potts model, this duality is expressed in terms of an electric-magnetic duality transformation, also called T-duality in the literature [29]. The T-duality relate the descriptions of the dilute and dense phase of the correspondent $O(n)$ model and it is at the basis of the Duplantier duality [4].

The natural question for the parafermions is then to see which are the relevant clusters. The answer, that we will explain in great details in this paper, is that i) the geometrical clusters percolate at the critical point and the associated exponents do not correspond to the corresponding model. ii) the FK clusters do **not** percolate at the critical point.

We will provide some details of the cluster algorithms that we employed in this study. Cluster algorithms have been first employed on the Potts model. The Potts model for any number of states is a two level local energy model on a lattice. The energy between two spins is either zero or a fixed value (β). Then the clusters are defined, for a fixed configuration of spins, as a problem of percolation. On all geometrical clusters which are build as neighboring spins taking the same value and connected with a term of energy β, one connects each pairs of spins with a probability $p = 1 - e^{-\beta}$. The resulting clusters of connected spins are the Fortuyin Kastelyn clusters which are used to build the dynamics of the model but also to measure observables like the magnetisation or the magnetic susceptibility.

For the $Z(N)$ parafermionic theory that we will consider here, the situation is more complicated. The local energy can take more than two values for $N \geq 4$ and a direct consequence is that the generalised clusters can connect spins with different values. Moreover, while for the Potts models it was possible to defined some quantities as the size of some FK clusters, this will not be the case here.

2 Definitions

One consider a model of spins variables S_i which can take N values, $S_i = 1, \cdots, N$ and are located on a square lattice of linear size L with periodic boundary conditions on both directions.

We consider the model defined on a square lattice with spin variable $S_j = \exp i2\pi/Nn(j)$ at each site j taking N possible values, $n(j) = 0, 1, \cdots, N-1$. The most general Z_N invariant spin model with nearest-neighbor interactions is defined by the reduced Hamiltonian [30, 31]:

$$H[n] = -\sum_{m=1}^{\lfloor N/2 \rfloor} J_m \left[\cos\left(\frac{2\pi mn}{N}\right) - 1 \right], \tag{2.1}$$

where $\lfloor N/2 \rfloor$ denotes the integer part of $N/2$. The associated partition function reads:

$$Z = \sum_{\{S\}} \exp\left[-\beta \sum_{<ij>} H[n(i) - n(j)] \right] . \tag{2.2}$$

For $J_m = J$, for all m, one recovers the $N-$state Potts model, invariant under a permutational S_N symmetry while the case $J_m = J\delta_{m,1}$ defines the clock model [32]. For $N = 2$ and $N = 3$ these models coincide with the Ising and the three-state Potts model respectively, while the case $N = 4$ is isomorphic to the Ashkin-Teller model [33, 34]. Defining the Boltzmann weights:

$$x_n = \exp\left[-\beta H(n)\right], \quad n = 0, 1, \cdots, N-1 , \tag{2.3}$$

the most general Z_N spin model is then described by $\lfloor N/2 \rfloor$ independent parameters x_n as $x_0 = 1$ and $x_n = x_{N-n}$. The general properties of these models for $N = 5, 6, 7$ have been studied long time ago (see e.g. [35] and references therein). The associated phase diagrams turn out to be particularly rich as they contain in general first-order, second-order and infinite-order phase transitions. For all the Z_N spin models it is possible to construct a duality transformation (Kramers-Wannier duality). In the self-dual subspace of (2.1)-(2.2), which also contains the Potts and the clock model, the Z_N spin model are critical and completely integrable at the points [36, 37] :

$$x_0^* = 1 \; ; \; x_n^* \;\; = \;\; \prod_{k=0}^{n-1} \frac{\sin\left(\frac{\pi k}{N} + \frac{\pi}{4N}\right)}{\sin\left(\frac{\pi(k+1)}{N} - \frac{\pi}{4N}\right)} . \tag{2.4}$$

There is strong evidence that the self-dual critical points (2.4), referred usually as Fateev-Zamolodchikov points, are described in the continuum limit by $Z(N)$ parafermionic theories [38]. Very recently, a further strong support for this picture has been given in [39] where the lattice candidates for the chiral currents generating the Z_N symmetry of the continuum model has been constructed.

3 Cluster algorithm

In this section, we explain how we can generalise the notion of FK clusters to the case of the Z_N spin model. We will consider configurations on a square lattice of linear size L with periodic boundary conditions for which we need to generate independant samples. The most convenient way to generate these samples is to use a cluster algorithm. The most effective cluster algorithm for discrete spin models is the Wolff [40] algorithm which

is based on the construction of the Fortyuin Kastelyn [41] clusters. We first recall how this algorithm works in the simple case of the N-states Potts model. Starting from

$$Z = \sum_{\{S\}} e^{\beta \sum_{<i,j>} \delta_{S_i S_j}} \ , \tag{3.1}$$

where the first sum $\{S\}$ is on all the spins $S_i = 1, \cdots, N$ while the second sum $< i, j >$ is on the first neighbor spins on the lattice, one easily gets

$$Z = \sum_{\{S\}} \prod_{<i,j>} e^{\beta \delta_{S_i S_j}} = (e^{\beta})^M \sum_{\{S\}} \prod_{<i,j>} ((1 - e^{-\beta})\delta_{S_i S_j} + e^{-\beta}) \ , \tag{3.2}$$

with M the total number of bonds on the lattice. Defining $p = 1 - e^{-\beta}$, the partition function is

$$Z = (e^{\beta})^M \sum_{\{S\}} \prod_{<i,j>} (p\delta_{S_i S_j} + (1 - p)) \ . \tag{3.3}$$

From there, one can read the rules to build the FK clusters. In a given configuration, for two neighbouring spins i and j such that $S_i = S_j$, one will put a bond with probability p and no bond with probability $1 - p$.

In the case of the parafermions the situation is a little bit more complicated. The partition function (2.2) can be written as

$$Z_N = \sum_{\{S\}} \prod_{<i,j>} (x_0^*)^{\delta_{n(i),n(j)}} (x_1^*)^{\delta_{n(i),n(j)\pm 1}} \cdots (x_{[N/2]}^*)^{\delta_{n(i),n(j)\pm [N/2]}} \ , \tag{3.4}$$

the delta function being defined modulo N, ie $\delta_{a,b} = 1$ if $a \equiv b \ (N)$. A decomposition similar to the one of (3.3) is

$$\begin{aligned} Z_N \ = \ & \sum_{\{S\}} \prod_{<i,j>} (1 - x_{[N/2]}^*)\delta_{n(i),n(j)} + (x_1^* - x_{[N/2]}^*)\delta_{n(i),n(j)\pm 1} \\ & + \cdots + (x_{[N/2]-1}^* - x_{[N/2]}^*)\delta_{n(i),n(j)\pm([N/2]-1)} + x_{[N/2]}^* \ . \end{aligned} \tag{3.5}$$

Note that due to the definition of the x_i^*, cf eq.(2.4), the x_i^*'s will be ordered and positives, $1 = x_0^* > x_1^* > \cdots > x_{[N/2]}^* > 0$. From there, one can read the construction of the generalised FK clusters. For each pair of neighbouring spins S_i and S_j, one will put a bond with probability

$$p_{|n(i)-n(j)|} = \frac{x_{|n(i)-n(j)|}^* - x_{[N/2]}^*}{x_{|n(i)-n(j)|}^*} \tag{3.6}$$

and no bond with probability $1 - p_{|n(i)-n(j)|}$. These FK clusters will be used to construct a cluster algorithm of Wolff type [40]. A lattice update consists in selecting one spin in the lattice at a random location then building the FK cluster containing this spin and then changing the color of this cluster by changing each spin of the lattice as $S_i \to S_i + j(N)$ with a random value $1 \leq j \leq N - 1$.

It is important to note that for the parafermions, the FK cluster will connect spins with different values which is not the case for the Potts model. One important consequence is that the resulting FK clusters can not be associated directly to some physical quantities like it was the case for the Potts models. For these models, the FK clusters

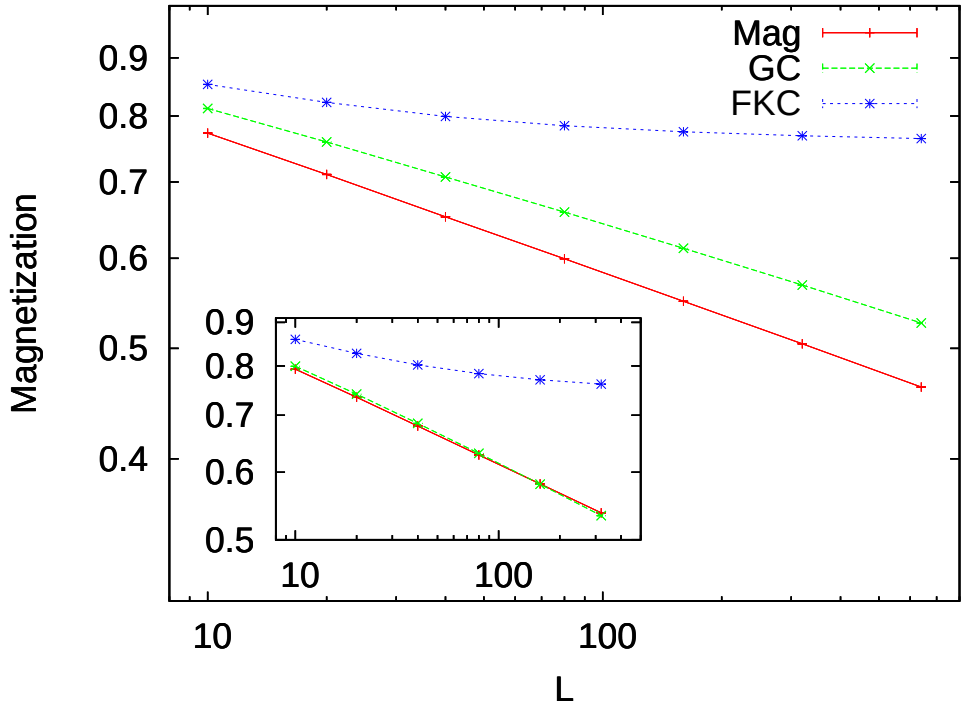

Figure 1: Main panel: Magnetization vs. L for the Z_4 spin model. The magnetization has been computed in three different ways: from eq. (3.7) and from the average of the largest geometrical and FK clusters. In the inset, the same plot for Z_5 spin model.

are the basic ingredient for building an update algorithm but they also encode all the informations associated to the critical behavior of the model under consideration. For example, the average size of a cluster build from a random site (Wolff algorithm) is equal to the magnetic susceptibility. Or the average size of the largest FK cluster divided by the volume is equal to the magnetization of the system. Or the two point spin-spin correlation function is equal to the probability that the two spins are in the same FK cluster. All these relation can not be valid any more in the case that we consider here. Still similar quantities can be defined. For example, if one defines for each cluster k

$$\rho_k = |\sum_i < e^{\frac{2i\pi n(i)}{N}} > | \,, \tag{3.7}$$

the sum being restricted to all the spins in the cluster k, then the magnetisation is associated to the maximum ρ_k along all the clusters. This is a simpler generalisation of the Potts model for which each FK cluster contains only spins with identical sign, thus in that case ρ_k is the volume of the FK cluster. We numerically compared the quantity $mag_1(L) = (\max(\rho_k)/L^2)$ with the real magnetisation obtained as a weighted sum on all the lattice

$$mag(L) = \frac{1}{L^2}|\sum_{i=1,L^2} < e^{\frac{2i\pi n(i)}{N}} > | \,, \tag{3.8}$$

the agreement being perfect for both the Z_4 and the Z_5 spin models. In the main panel of Fig.1, we plot for the Z_4 spin model, the magnetisation obtained from eq. (3.7)

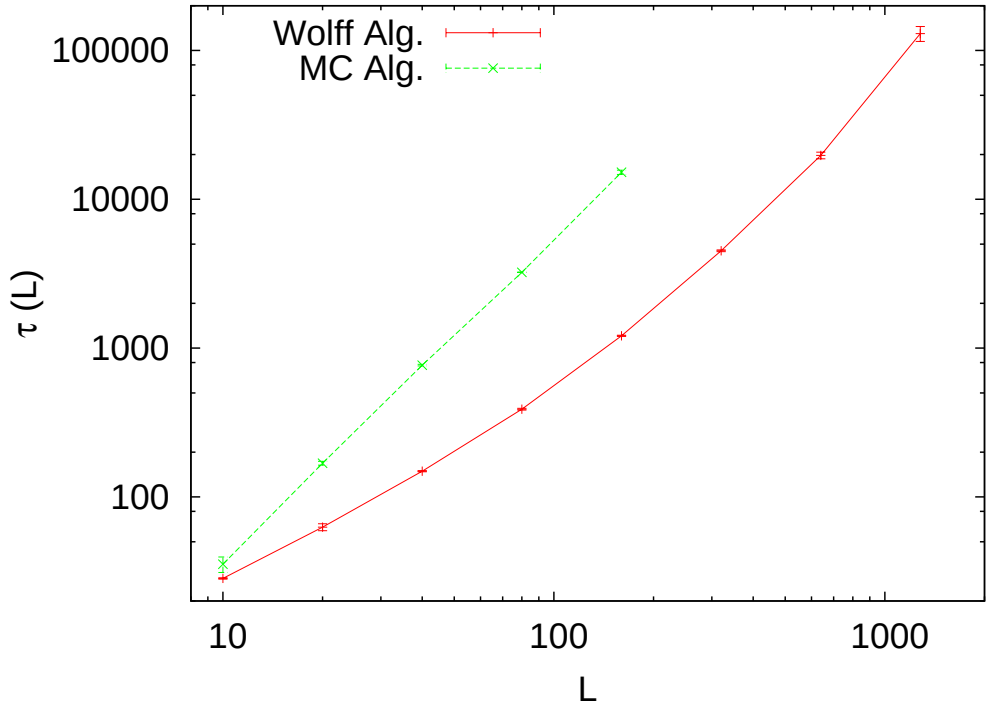

Figure 2: Autocorrelation time vs. L for the Z_4 spin model. We show the data for the Wolff algorithm as well as for ordinary Monte Carlo updates. The Wolff algorithm show a much better efficiency in the range of lattice sizes explored.

which is compared to the value of the average largest FK cluster and the average largest geometrical cluster (in both cases divided by L^2). The scaling is perfect for the magnetization given by eq. (3.7) with an exponent in very good agreement with the expected one, $\beta/\nu = 1/8$ [36]. For the geometrical cluster, we also observe a good scaling but with stronger finite size corrections. Due to these corrections, it is difficult to give a definite exponent associated to the geometrical clusters, we obtain for the largest sizes $\beta/\nu = 0.110(1)$. Since this value is increasing with the size, one can speculate that in the infinite size limit this value will converge towards the magnetic exponent β/ν. We also observe that the largest FK cluster will occupy a finite fraction of the lattice in the large size limit, which corresponds to the case where the percolation threshold has been exceeded. We will come back on this point in the next section.

In the inset of Fig.1, we show similar data for the Z_5 spin model. We also obtain an excellent agreement between the exponent obtained from eq. (3.7), the real magnetisation eq. (3.8) and the exact result $\beta/\nu = 4/35$ [36]. We see that the geometrical cluster exponent is again affected by strong finite size effects and it will become larger than the magnetic exponent already for the simulated sizes (note the crossing between this curve and the one corresponding to the magnetization from eq. (3.7)). As for the Z_4 case, the largest FK cluster do not present a scaling law at the critical point.

Even if we expect that the FK clusters are not the natural object to compute the critical exponents of the Z_N spin models, we can still use them to build cluster algorithms. In Fig. 2 we plot the autocorrelation time for the Wolff algorithm in the Z_4 spin model

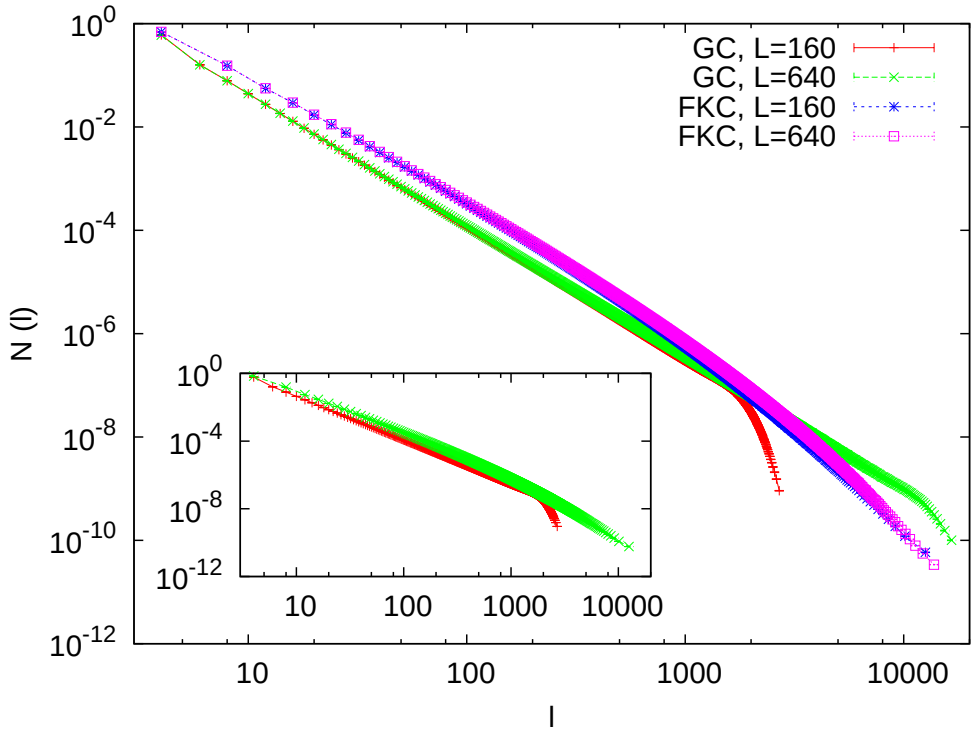

Figure 3: Distribution of cluster lengths for the Z_4 spin model and different lattices sizes. While the geometrical clusters show a nice power law distribution, the FK cluster distribution falls away from a power law. In the inset, we show similar data for the Z_5 spin model and $L = 160$.

and we compare it to the autocorrelation time for standard heat bath Monte Carlo. We observe that the Wolff algorithm is much more effective than the Monte Carlo one. The autocorrelation time for the Monte Carlo algorithm scales as $\tau(L) \simeq L^{z_{MC}}$ with $z_{MC} = 2.1(1)$. The dynamical exponent z is much smaller for the Wolff algorithm at small sizes ($z_W \simeq 1.2(1)$) but then it increase for larger sizes. This effect will be explained in the next section. For the sizes that we can simulate, $L \leq 1280$, the Wolff algorithm will always be more efficient than Monte Carlo. This is also the case for the Z_5 spin model.

4 Percolation and critical properties

In this section, we present results for the properties of both geometrical and FK clusters in the Z_4 and Z_5 spin models. We show that the distribution of cluster lengths in the critical point is a power law for geometrical clusters but not for FK clusters. Furthermore we show that the geometrical clusters percolate at the critical point, while the FK clusters do not. We also perform a first determination of the fractal dimension of the geometrical clusters by using the exponent associate to the distribution of cluster lengths.

First, we consider the distribution of the length [1] of contours for the finite size clusters

[1] As explained in the next section, there exist two natural ways to define a length. Both methods

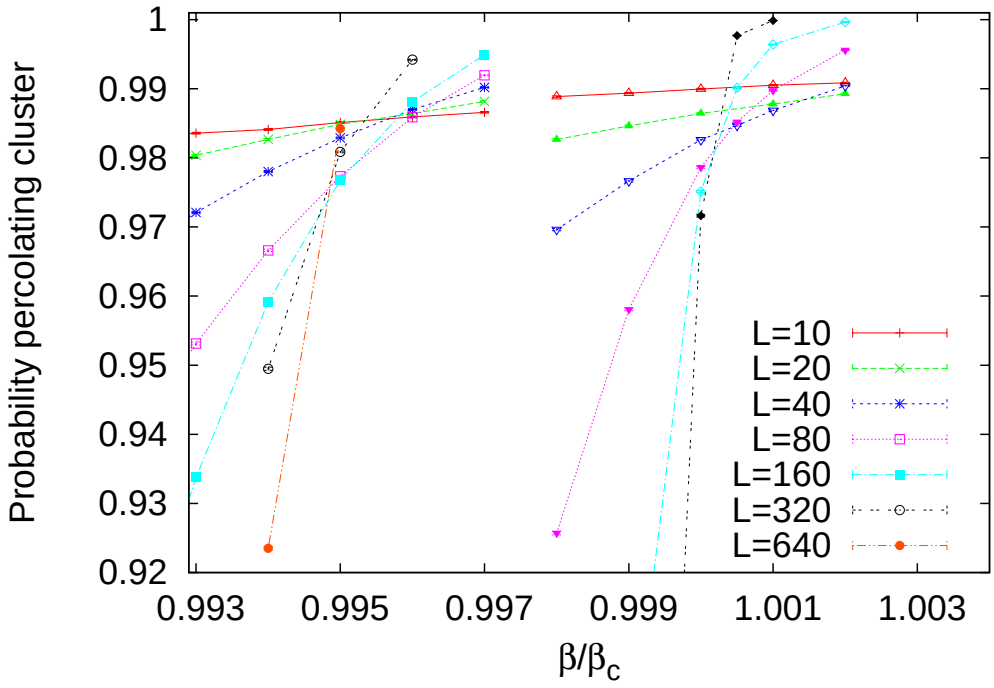

Figure 4: Percolation test for Z_4 spin model. The right part corresponds to the geometrical clusters, which percolate right at the critical point. The left corresponds to the FK clusters, which do not percolate at this point.

at the critical point. In Fig.3, we present this distribution for both geometrical and FK type of clusters in the Z_4 spin model for $L = 160$ and 640. For both lattice sizes, we observe a nice scaling for the geometrical clusters with a distribution which is well described by a power law $N(l) \simeq l^{-\tau_g}$ characteristic of a percolation critical point [42] with $\tau_g \simeq 2.5(1)$. We expect that τ_g is related to the fractal dimension by the following relation $d_f = 2/(\tau_g - 1) \simeq 1.33(10)$ which is of the same order of what is measured in the SLE context [22, 23]. In the next section, we will present more precise measurements for the fractal dimensions of the geometrical clusters. For the FK clusters, it is clear that the scaling is not satisfied. The distribution is better described by $N(l) \simeq l^{-\tau_{fk}} \exp(-l/\xi)$ with some finite correlation length ξ with a value of order 2500 lattice units for the Z_4 spin model.

This provides a first evidence that the FK clusters do not percolate at the critical point of the Z_4 spin model. This is confirmed in Fig.4, where we present the probability of having a percolating cluster vs. the ratio β/β_c (which measures the distance to the critical point), for both the geometrical and the FK clusters. The probability is computed for increasing lattice sizes. Converging crossing points indicate a critical point. This is clearly observed for the geometrical clusters with a critical point close to $\beta = \beta_c$. For the FK clusters we do not observe a clear convergency and the lines cross around $\beta \simeq 0.995\beta_c$. This corresponds to the finite correlation length previously observed for the distribution of FK clusters length. To convince the reader that such a small deviation,

converge to the same result in the large size limit.

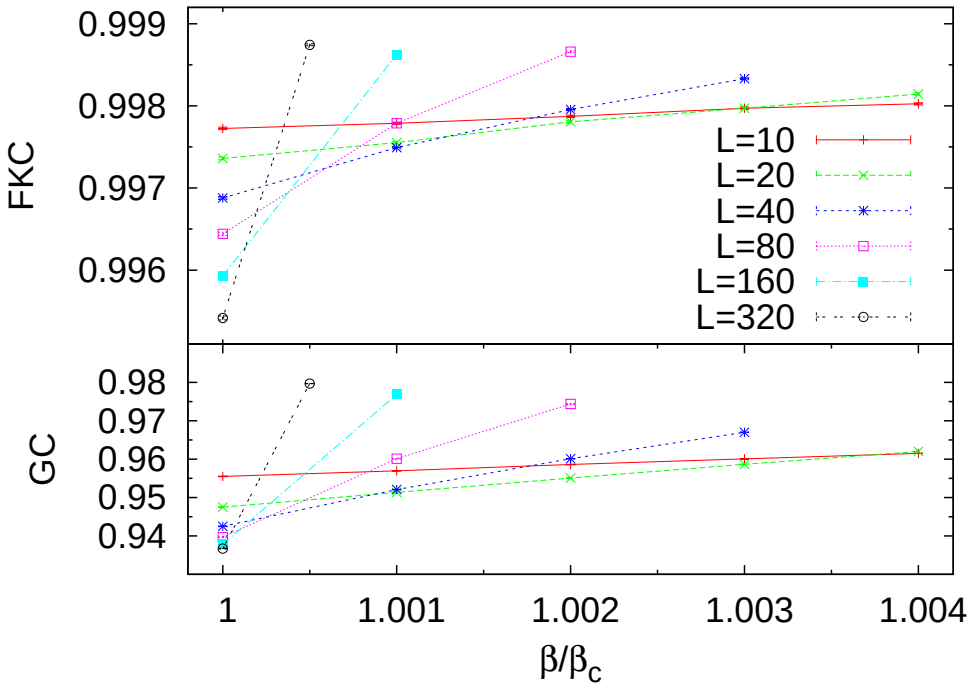

Figure 5: Percolation test for 3-states Potts model. The upper part corresponds to the FK clusters, while the lower part corresponds to the geometrical clusters. Both types of clusters percolate at the critical point.

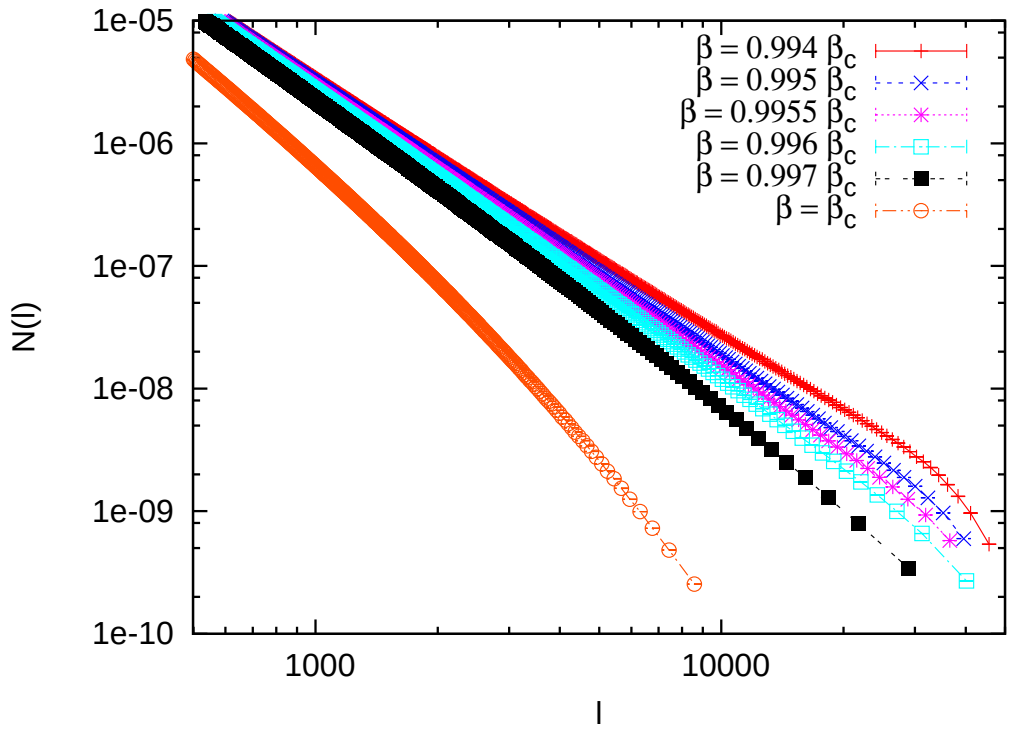

Figure 6: Distribution of FK cluster lengths for the Z_4 spin model and $L = 320$ for different values of the parameter β very near the critical point.

$|\beta - \beta_c|/\beta_c \simeq 0.005$, is in fact important, we show in Fig.5 a comparative plot for the 3-states Potts model. For this model, both types of clusters percolate at β_c. For the larger lattice size, we see that the deviation is near two order of magnitude smaller than it was for the Z_4 spin model. The percolation value $\beta \simeq 0.995\beta_c$ is also confirmed in Fig. 6 where we plot the distribution $N(l)$ of the FK clusters for various value of β and for $L = 320$. We observe a nice power law close to $\beta = 0.995\beta_c$.

In the case of the Z_5 spin model we obtain similar results. The distribution of geometrical cluster lengths shows a power law scaling, while the length distribution of FK clusters presents a finite correlation length ξ with a value of order 5000 lattice units. See the inset of Fig. 3. Furthermore, geometrical clusters percolate right at the critical point $\beta = \beta_c$, while FK clusters percolate at $\beta = 0.9975\beta_c$.

5 Fractal dimensions in the bulk

In this section we present a more accurately computation for the fractal dimensions of the geometrical clusters for both Z_4 and Z_5 spin models.

As explained in the previous section, the fractal dimension can be obtained from the distribution $N(l) \simeq l^{-\tau}$ via the relation $d_f = 2/(\tau - 1)$. This method turns out not to be very precise since there exist very strong finite size corrections in the determination of τ. Here we present another method which provides a better precision by computing the average area of the cluster as a function of the interface length around the cluster.

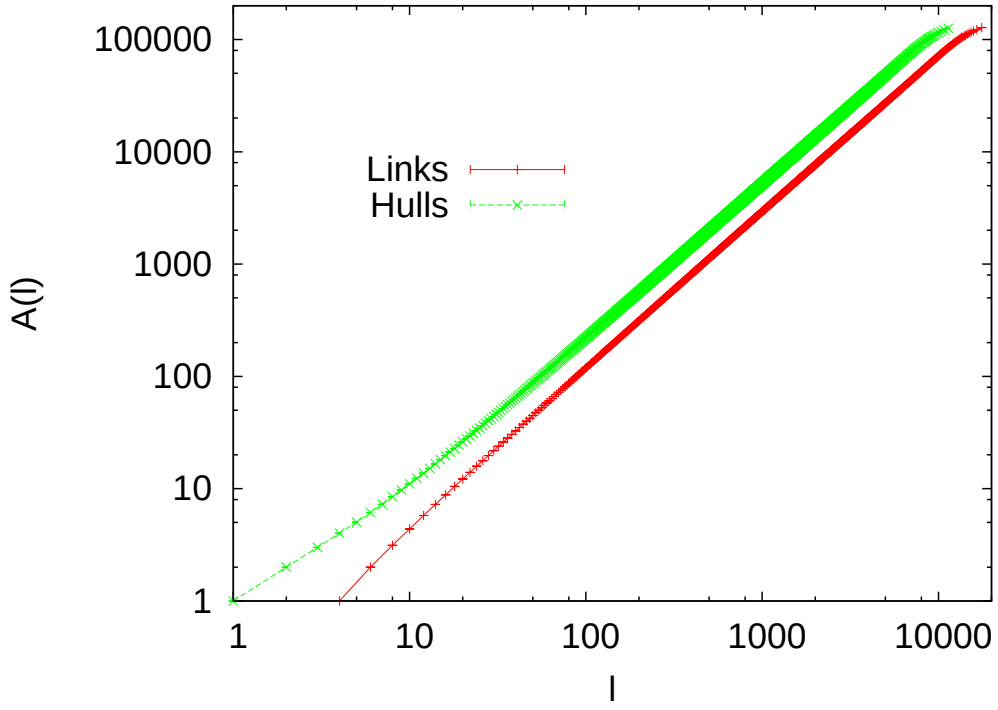

Figure 7: $A(l)$ vs. l for the two definitions of the length (links and hulls, see text for details) on the geometrical clusters of the Z_5 spin model.

We will consider two different definitions of the cluster interface length. The first one, which we will call the *link length* corresponds to the number of bonds which are broken around the cluster. For example, for one isolated spin, the length is $l_l = 4$. The second definition, which we will call the *hull length*, counts the number of spins on the border of the cluster. For an isolated spin, one has $l_h = 1$.

The fractal dimension is defined as $l = R^{d_f}$ with R the radius of gyration of the cluster. A more direct measurement is given by computing the average area as a power law of l with $A(l) = R^2 \simeq l^{2/d_f}$. In Fig. 7 we show the data for the Z_5 spin model. In this plot, we present $A(l)$ for two definitions of l, the hull and the link one. We get a nice scaling law over a large range of l's. The asymptotic limit is similar for the two definitions of lengths (hulls and links). A fit of the data gives a value of $d_f \simeq 1.44(1)$, but such a fit does not provide a good precision since it is very difficult to take in account the small and large size corrections. Note that there is a bending in both of these curves for small sizes. These bendings, which are due to small size corrections, are in opposite directions for the two definitions of lengths that we employ. This fact will be very useful for the extraction of a precise fractal dimension and motivate the measurement of the two lengths.

A better estimate is obtained in the following way: in Fig. 8 we show a similar plot after a rescaling $l \to l/L^{d_f}$ and $A(l) \to A(l)/l^{2/d_f}$. The rescaling is motivated by the fact that L^{d_f} corresponds the length of a cluster who fills the lattice, *i.e.* $A = (L^{d_f})^{2/d_f} = L^2$. We observe a collapse for the large size clusters. There still exists strong finite size corrections, for both small and large cluster lengths, but we see that a plateau appears

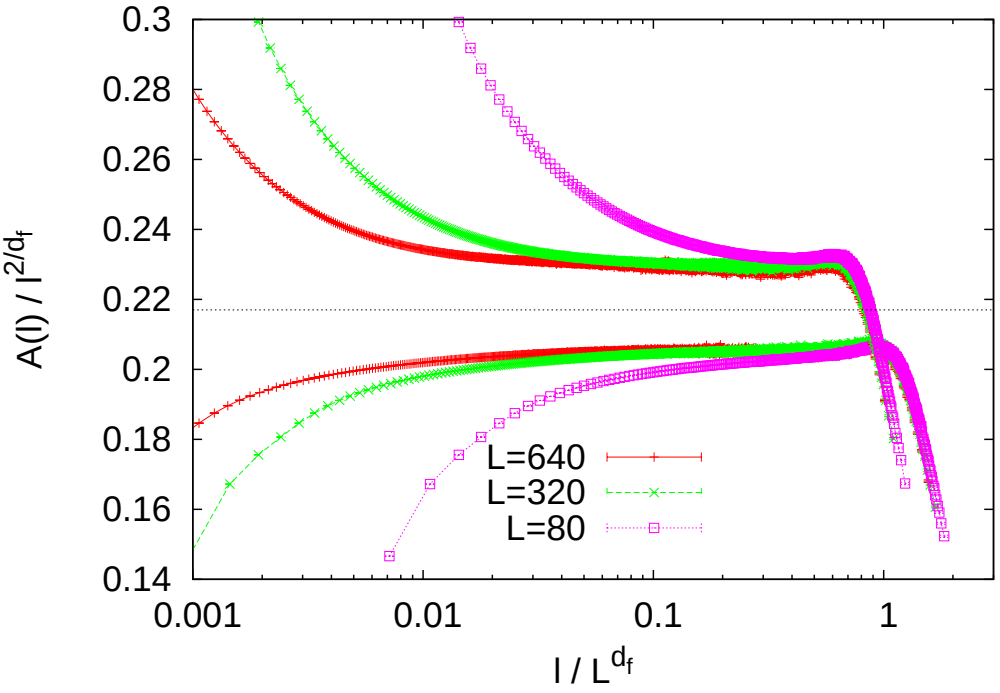

Figure 8: Rescaling for the Z_5 spin model and different system sizes with $d_f = 1.446$. The upper curves correspond to the hull lengths with the lower ones correspond to the link lengths.

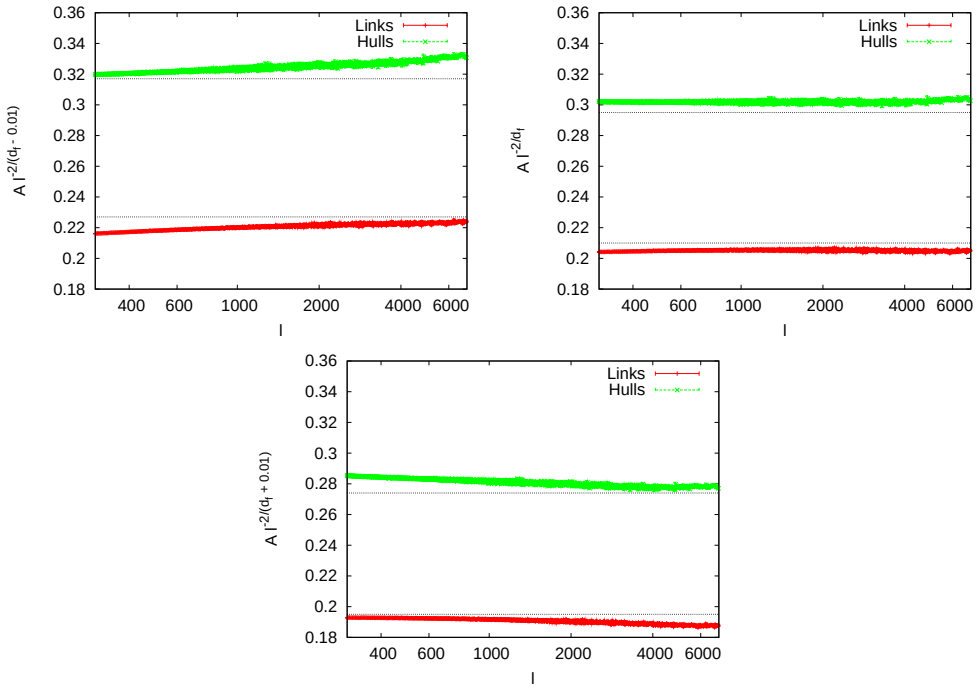

Figure 9: Comparative with three values $d_f - 0.01$, d_f and $d_f + 0.01$ for $L = 640$ in the Z_5 spin model with $d_f = 1.450$ for the hull cluster length and $d_f = 1.444$ for the link cluster length. This plot show the accuracy on the determination of the fractal dimension.

which correspond to the region where scaling works. The optimal values are $d_f = 1.450(2)$ for hulls and $d_f = 1.444(2)$ for links. In Fig. 9 we check the accuracy of our estimation for the Z_5 fractal dimension. By plotting $A/l^{2/d_f}$ vs. l, the good value of the fractal dimension should correspond to straight and perfectly horizontal lines. As shown in the figure, this is obtained for an optimal value of $d_f = 1.446(2)$ (which correspond to the average of hull and link fractal dimension).

For the Z_4 spin model, we can perform similar measurements. We show in Fig. 10, values obtained for d_f for Z_4 and Z_5 and for both definitions of the length. This figure contains the main results of our work. As a final result for the fractal dimension of the geometrical clusters, we obtain $d_f = 1.438(2)$ for the Z_4 spin model and $d_f = 1.446(2)$ for the Z_5 spin model.

6 Summary and conclusions

In this paper we studied by Monte Carlo methods the geometrical properties of the Z_N spin model. The samples were generated by using a cluster algorithm which generalize the notion of FK clusters to the case of the Z_N spin model. For $N \geq 4$ the FK clusters will in general connect spins with different values. This is not the case for $N = 2$ and $N = 3$, respectively the Ising and three-states Potts model. The cluster algorithm allows to track both geometrical and FK clusters and the distribution of all the finite closed geometrical and FK clusters can be studied.

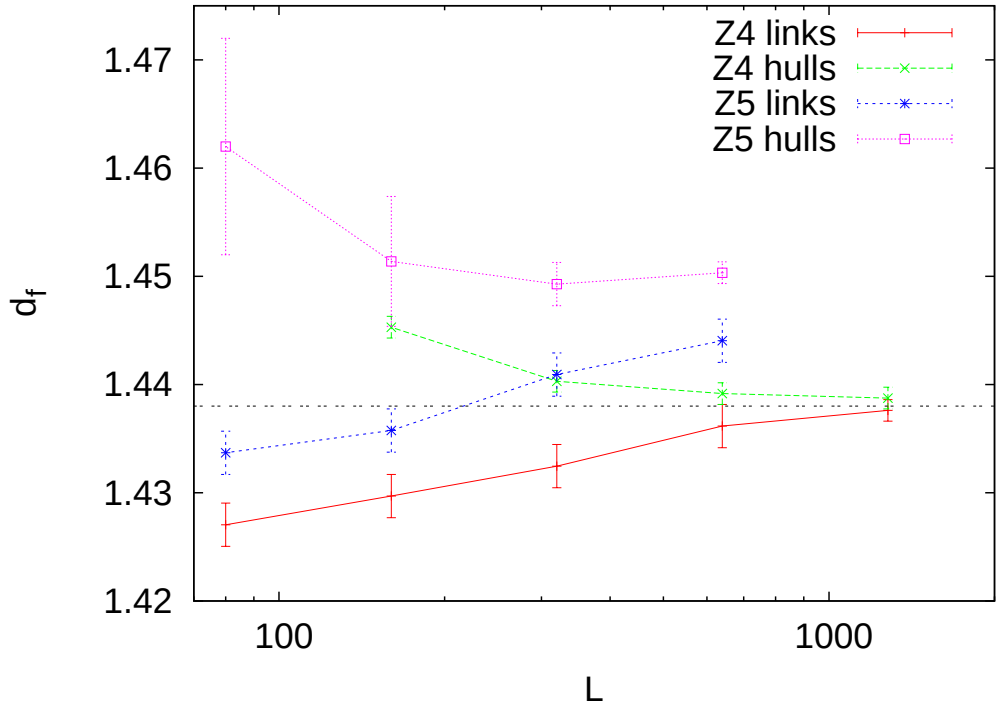

Figure 10: Estimations of the fractal exponents for both hull and link lengths, in the Z_4 and Z_5 spin models as a function of the lattice size.

In particular we have shown that the geometrical clusters percolate at the critical point and the associated exponents do not correspond to the exponents given by the unitary Kac table of the associated Z_N parafermionic field theory. Note that this is also true for the geometric clusters for $N = 2, 3$. We have determined the fractal dimension of the boundaries (interface) of the geometric clusters. By measuring the distribution in size and area of the geometrical clusters, we determined the fractal dimension $d_f = 1.438(2)$ for $N = 4$ and $d_f = 1.446(2)$ for $N = 5$. It is important to note that these values are different from the ones proposed by one of the authors in [21] for SLE interfaces in parafermionic theories and measured numerically for some particular type of boundary condition in [22]. Still the fractal dimension obtained by numerically studying interfaces related to certain different types of boundary conditions are in good agreement with the one determined here in the bulk [23].

We have also shown that, although the cluster (Wolff) algorithm show a much better efficiency in the range of system lengths studied, the FK clusters do **not** percolate at the critical point for $N \geq 4$. This is the reason while computed the fractal dimension only for the geometrical clusters.

The results we obtained point out important differences in the behavior of the geometrical and FK clusters between the case $N = 2, 3$, where the system can be described by a minimal CFT model, and the case $N \geq 4$, described in the continuum limit by an extended CFT. This can be traced back to the fact that, for $N \geq 4$ the internal Z_N degrees of freedom play a fundamental role. This calls for further analytical studies of the bulk geometric properties of the parafermionic theories. One way to tackle this problem

would be to provide a Coulomb gas description for parafermionic theories which would allow to identify the operators associated to the geometric interface and to compute the associated fractal dimensions.

Acknowledgments

We thanks Benoit Estienne for useful discussions. This work has been done in part when one of the authors (RS) was guest of the Galielo Galilei Institute in Florence, whose hospitality is kindly acknowledged.

References

[1] see for instance B. Duplantier, Les Houches 2005 Lecture Notes, Session LXXXIII, 101, Elsevier (2006), math-ph/0608053

[2] B. Nienhuis, in *Phase Transitions and Critical Phenomena*, edited by C. Domb and J. L. Lebowitz (Academic, London, 1987), Vol. 11, p.1.

[3] H. Saleur and B. Duplantier, *Phys. Rev. Lett.* **58**, 2325 (1987).

[4] B. Duplantier, *Phys. Rev. Lett.* **84**, 1363 (2000).

[5] W. Kager and B. Nienhuis, *J. Stat. Phys.* **115**, 1149 (2004).

[6] J. Cardy, *Annals Phys.* **318**, 81 (2005).

[7] M. Bauer and D. Bernard, *Phys. Rept.* **432**, 115 (2006).

[8] M. Bauer and D. Bernard, *Comm. Math. Phys.* **239**, 493 (2003).

[9] M. Bauer and D. Bernard, *Phys. Lett.* **B543**, 135 (2002).

[10] M. Bauer and D. Bernard, *Phys. Lett.* **B557**, 309 (2003).

[11] I. Affleck and F. D. M. Haldane, *Phys. Rev.* **B36**, 5291 (1987).

[12] A. W. W. Ludwig, *Nucl. Phys.* **B285**, 97 (1987).

[13] V. Dotsenko, M. Picco and P. Pujol, *Nucl. Phys.* **B455**, 701 (1995).

[14] J. Rasmussen, hep-th/0409026.

[15] E. Bettelheim, I. A. Gruzberg,A. W. W. Ludwig and P. Wiegmann, *Phys. Rev. Lett.* **95**, 251601 (2005).

[16] V. Pasquier, *Nucl. Phys.* **B285**, 162 (1987).

[17] P. Di Francesco, H. Saleur and J.-B. Zuber, *Nucl. Phys.* **B300**, 393 (1988).

[18] P. Fendley, *J. Phys.* **A39**, 15445 (2006).

[19] Y. Ikhlef and J. Cardy, arXiv:0810.5037.

[20] M. A. Rajabpour, *J. Phys.* **A41**, 405001 (2008).

[21] R. Santachiara, *Nucl. Phys.* **B793**, 396 (2008).

[22] M. Picco and R. Santachiara, *Phys. Rev. Lett.* **100**, 015704 (2008).

[23] M. Picco and R. Santachiara, in preparation.

[24] A. Gamsa and J. Cardy, *J. Stat. Mech.* P08020 (2007).

[25] A. Coniglio, C. Nappi, F. Perrugi and L. Russo, *J. Phys.* **A10**, 205 (1977).

[26] M. F. Sykes and D. S. Gaunt *J. Phys.* **A9**, 2131 (1976).

[27] H. Müller-Krumbhaar, *Phys. Lett.* **50A**, 27 (1974).

[28] Vl. S. Dotsenko, G. Harris, E. Marinari, E. Martinec, M. Picco and P. Windey, *Nucl. Phys.* **B448**, 577 (1995).

[29] I. Rushkin, E. Bettelheim, I. A. Gruzberg and P. Wiegmann, *J. Phys.* **A40**, 2165 (2007).

[30] A. B. Zamolodchikov, *Zh. Eksp. Teor. Fiz.* **75** (1978), 341 [*Sov. Phys. JETP* **48**, 168 (1978)].

[31] V. S. Dotsenko, *Zh. Eksp. Teor. Fiz.* **75** (1978), 1083 [*Sov. Phys. JETP* **48**, 546 (1978)].

[32] F. Y. Wu, *Rev. of Mod. Physics* **54**, 235 (1982).

[33] J. Ashkin and E. Teller, *Phys. Rev.* **64**, 178 (1943).

[34] K. .Y. Lin and F. Y. Wu, *J. Phys.* **C7**, L181 (1974).

[35] F. C. Alcaraz and R. Köberle, *J. Phys.* **A14**, 1169 (1981).

[36] V. A. Fateev and A. B. Zamolodchikov, *Phys. Lett. JETP* **92A**, 37 (1982).

[37] F. C. Alcaraz and R. Köberle, *J. Phys.* **A13**, L153 (1980).

[38] F. C. Alcaraz, *J. Phys.* **A20**, 2511 (1987); *J. Phys.* **A20**, 623 (1987).

[39] M. A. Rajabpour and J. Cardy, arXiv:0708.3772

[40] U. Wolff, *Phys. Rev. Lett.* **62**, 361 (1989).

[41] C. M. Fortuin and P. W. Kasteleyn, *Physica* **57**, 536 (1972).

[42] D. Stauffer and A. Aharony, Introduction to Percolation Theory, 2nd edition (Taylor and Francis, London, 1994).